GEOLOGICA CARPATHICA – SERIES CLAYS, 6, 1, BRATISLAVA, JUNE 1997
11 – 25

NEW DATA ABOUT THE HALLOYSITE FROM ANGLEUR TYPE-LOCALITY, BELGIUM

ERIC GOEMAERE[1] and ALAIN HANSON[2]

[1] Liège University, Clay Geology Laboratory, Boulevard du Rectorat, Batiment B18, Sart Tilman, 4000 Liège, Belgium
[2] Fondation Universitaire Luxembourgeoise, Avenue des Déportés, 6700 Arlon, Belgium

(Manuscript received February 4, 1997; accepted in revised form May 19, 1997)

Abstract: New samples of halloysite from the type-locality of Angleur were investigated. X-ray, chemical, optical, and thermal analyses of this halloysite show a strict relation of hydration with a continuous transition from halloysite-(10 Å) to halloysite-(7 Å). Oxydation of a sulfide orebody associated with the Streupas fault is taken as the main source for acids which have played a role in the karstification of Tournaisian dolomitic limestones and in the halloysite genesis. The source-rock for Al and Si is derived from leaching of illites from Namurian black shales.

Key words: halloysite, variable hydration rate, chemical and physical properties (XRD, DTA, TGA, Infrared spectroscopy, CEC), optical properties, karstification, associated minerals (viseite, alumohydrocalcite, allophane, gibbsite).

Introduction

Originally discovered by J J. d'Omalius d'Halloy (1783–1875) in Angleur locality, near Liège (Fig. 1) at the beginning of the 19th century, the mineral has been subsequently named halloysite by Berthier (1826) on the basis of its megascopic properties and chemical composition. Additional chemical data were added by Le Châtelier (1887), Splichal (1919), Ross & Kerr (1935) and Buttgenbach (1947). Optical properties and powder diffraction data were only reported by Ross & Kerr (1935), and De Keyser & Degueldre (1954). The present review completes former investigations and provides up-to-date data about Angleur's halloysite.

In order to avoid ambiguous names or terms, Giese's nomenclature (1988) has been adopted. Therefore, the name «halloysite» will be used as a generic term. The state of hydration will be specified by appending the d(001) value as in «halloysite-(10 Å)» for fully hydrated phase.

The study area is located at the southeastern border of the Namur Synclinorium where thrustwedges were pinched in the Condroz overthrust. In the vicinity of the Liège locality (L in Fig. 1), Streupas and Kinkempois thrustwedges constitute the Angleur promontory between the Meuse and the Ourthe valleys (Fig. 1). This promontory is composed by Upper Devonian and Carboniferous strata bordered by the Eifelian Fault to the South, and is separated from the Liège Namurian coal basin by the Streupas and Kinkempois mineralized faults to the North. Sphalerite–galena–pyrite ore bodies were intensively mined during the 18th and 19th centuries. Maps of the Diguette underground mine show that the ore deposits consisted of small sulfide pockets, lined up along the Streupas fault, and exclusively concentrated in the dolomitized crinoidal Tournaisian limestone, at the contact with slightly pyritous Namurian black shales. Angleur promontory has been covered by sands accumulated during the Oligocene transgression, and finally by Meuse terrace sediments. Details about the geology of the area were given by Lambrecht (1958), Lambrecht & Swinnen (1958), Swinnen (1958), and Calembert et al. (1974).

Experimental and material

Halloysite and limonitised limestone were recently sampled from solution cavities related to the gossan where halloysite was originally studied (Berthier 1826; Davreux 1833). Unfortunately, the extent of the now closed mine and karstic phenomena in the prospected area mask clear geological relations. Nevertheless, the collected samples were located at the contact between halloysite and enclosing materials.

Only isolated milky or yellowish brown fragments of a clayey material in which halloysite was the major component were observed. Two types of halloysite were macroscopicaly distinguished in all the collected samples. They are similar to those described by Ross & Kerr (1935) and presently assembled at the Institute of Mineralogy of Liège University since the 19th century.

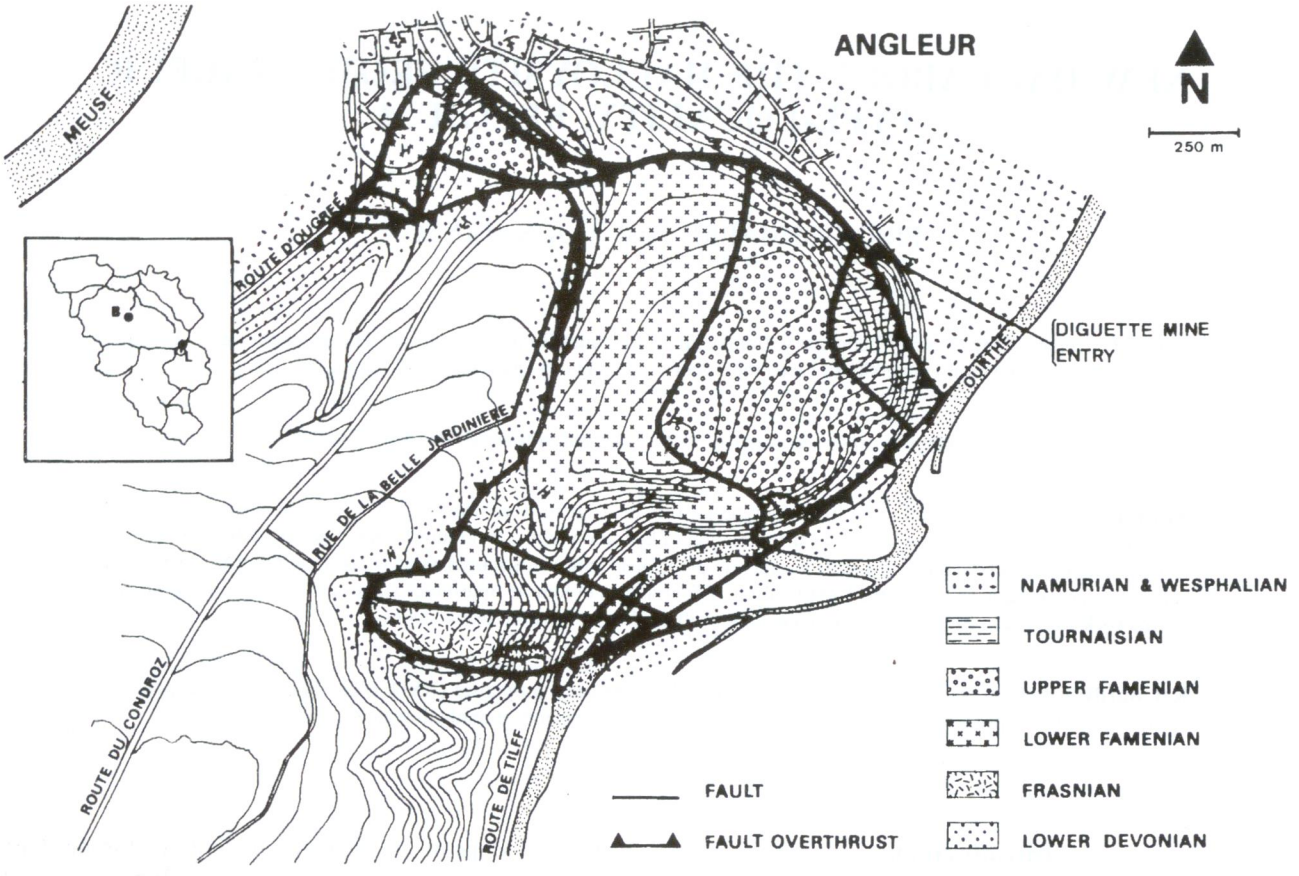

Fig. 1. Sketch map of the Angleur promontory. Geographic and geologic location of halloysite samples. B: Bruxelles; L: Liège; circle: location of Angleur area.

One sample consisted of pale blue, waxy, porcelaneous, pure botryoidal masses breaking with a conchoidal fracture, and cracking upon drying into white angular fragments (Type–I). This material matched Berthier's (1826) original description and was called «boule de suif» by Davreux (1833). Another sample was white, cottony, chalky, porous (Type–II), and formed powdery heterogeneous clusters. Several samples showed a core of bluish halloysite (Type–I) wrapped in a mixture of white halloysite (Type–II) often stained by iron hydroxides with gibbsite, alumohydrocalcite, viseite and/or allophane. Relationships between Type–II halloysite and other minerals identified by X-ray diffraction and SEM have shown that: — glassy black allophane and gibbsite form thin seams of reticulating Type–II halloysite (see below); — gibbsite crystals, up to 0.5 mm across also were found in vugs and fractures of Type–II halloysite and allophane; — viseite spherules constituted of discoidal platy crystals (0.01 mm) occurred in association with gibbsite; — alumohydrocalcite formed radiating aggregates of up to 1 mm long silky white needles in vugs.

X-ray powder diffraction patterns were obtained with a Phillips (PW 1730) diffractometer, with Ni-filtered Cu Kα radiation (30 KV, 30 mA, time constant = 2 sec., paper speed 2 cm/min., scan rate of 1 or 2°2θ/min., sensitivity = 10^3 or 2.10^3 impulse/sec). The following XRD method was applied for 40 recently collected specimens. Samples were dried at room temperature, gently crushed and homogenized in hand mortar. The finely ground powder was then mounted in a shallow cavity of the glass slide support, in order to minimize any preferred orientation, and X-rayed from 2° to 65°2θ. The powder was afterwards put in suspension in deionized water without any ultrasonic desaggregation. A well dispersed < 10 μm size fraction was obtained by sedimentation and transferred as dilute aqueous suspensions onto a glass slide. XRD patterns were recorded to complete the formerly published XRD data of halloysite from Angleur. Oriented aggregates were: a) dried at room temperature with relative humidity monitoring (N); b) saturated overnight with ethylene-glycol vapors (EG); c) heated to 110 °C for 4 hours (Q 110), 300 °C for 2 hours (Q 300); and d) and to 500 °C for 4 hours (Q 500).

Four halloysite samples exhibiting typical XRD patterns were post-treated with dimethylsulfoxide G.R. (DMSO), formamide G.R., hydrazine vapors, and boiling with HCl 4N (5 minutes). Each sample was air dried, then treated in closed vessel for 18 hours with DMSO vapors at 60 °C or with formamide vapors at 30 °C, heated to 110 °C for 2 hours, and again solvated with DMSO or formamide re-

Table 1: Chemical analyses of Angleur's halloysite.

N°	(1)	(2)	(3)	(4)	(5)	(6)	(7)
P_2O_5	—	—	—	—	0.04	0.08	0.02
SiO_2	39.5	42.4	44.75	37.7	39.58	41.67	44.32
TiO_2	—	—	—	—	0.00	0.03	0.02
Al_2O_3	34.0	36.1	36.94	38.5	33.82	34.65	35.15
Fe_2O_3	—	—	—	2.3	0.02	0.10	0.10
MnO	—	—	—	—	0.00	0.01	0.01
ZnO	—	—	—	—	0.18	0.11	0.10
CaO	—	—	0.11	—	0.18	0.15	0.16
MgO	—	—	—	—	0.03	0.02	0.02
Na_2O	—	—	0.91	—	0.01	0.00	0.01
K_2O	—	—	0.91	—	0.01	0.00	0.00
H_2O_{Tot}	26.5	21.6	17.42	21.4	26.05	23.40	19.63
TOTAL	100.0	100.0	100.13	99.9	99.92	100.22	99.54

(1) Berthier 1826
(2) Le Chatellier 1887
(3) Richardson in Ross & Kerr 1935
(4) Buttgenbach 1947
(5) Type-I: blue, porcelaneous (this work) (Ni= 156 ppm; Cr= 169 ppm; Co= 55 ppm)
(6) Blue-greyish halloysite (this work)
(7) Type-II: white, terrous (this work)

spectively. For hydrazine saturation, each sample was air dried, treated with hydrazine vapors at 40 °C for 6 days, then at 50 °C for one day, and finally air dried one night (dehydrazination).

For chemical analyses, the material was hand picked under a 50X binocular microscope; only the homogeneous material, free of contaminents has been investigated. Beside wet chemical analysis data compiled from literature, new data for three newly collected samples were obtained (Table 1). Analyses were performed using standard analytical methods: Si, Al, Fe, Mn, Zn, Mg, Ca, K and Na by A.A.S.; P by colorimetry; H_2O by L.O.I. and T.G.A.

Dehydration curves of halloysites exhibiting different hydration rates were obtained from 35 mg of sample, by using a SETARAM 1972 (LA 162) microthermobalance. The automatic heating device was run from 25 to 1000 °C.

The IR spectra (Fig. 9) were recorded with a Beckman IR 4250 spectrophotometer in the 300–4000 cm^{-1} region, 2 mg of samples having been prepared by the conventional KBr pressed pellets technique.

Optical properties were determined by the double variation method, a few seconds after the sample had been freed of water and slightly crushed.

Experimental data and discussion

1. X-ray powder diffraction

Although data were abundant in the literature about the X-ray properties of halloysites with different morphologies and from various deposits, X-ray data of halloysite from the type-locality of Angleur were restricted to a single list of d(hkl) spacings obtained from powdered samples with no further specific chemical composition.

The X-rayed powder patterns have shown mainly halloysite with minor gibbsite, alumohydrocalcite, viseite and quartz in decreasing order of abundance. Fig. 2 presents the XRD patterns of powdered samples in order of decreasing hydration (samples 2–6–7–8). In many XRD patterns, an increase of background gave rise to a plateau between 23° and 40°2θ, indicating allophane admixture.

Sample 2 corresponded to nearly a fully hydrated halloysite-(9.9 Å) in Angleur deposit, and was named Type–I. It was characterized by an intense (001) peak at 9.9 Å, a less intense peak (11–,02–) and weak to poorly resolved XRD reflections at 3.34 Å, 2.55 Å, 2.33 Å, 1.67 Å and 1.47 Å.

Type–II halloysite (samples 6 and 7) exhibited a sharp decrease of height/width ratio together with a progressive shift of (001) towards 7.49 Å typical for an intermediate state of dehydration.

Halloysite 7 was the most naturally dehydrated sample whereas halloysite 6 corresponded to a partially dehydrated halloysite with a broad diffraction band extending between 10 and 7.49 Å. This band resulted from random or to partially random mixed-layering of hydrated and dehydrated layers. When halloysite lost its interlayered water, the shift of (001) was conterbalanced by an increase of the (hkl)/(001) intensity ratio.

Althought a completely dehydrated halloysite has not been found in Angleur, sample 8, originally of Type–I (Liège University Mineralogical Museum), actually matched Type–II. Its XRD pattern had the characteristics of a dehydrated end member, and exhibited a single broad reflection centered at 7.49 Å, with a slight asymmetry on the low angle side. This agreed with the following observation: halloysite-(10 Å) easily and rapidly loses its interlayer water under ambient conditions and even samples stored under saturated water vapor or in liquid water may still dehydrate (Giese 1988).

2. X-ray diffraction of oriented agregates

Routine XRD analysis was applied to five samples prepared as oriented aggregates in order to illustrate the hydration behaviour (Fig. 3). Air dried (or natural = N) samples offered XRD patterns similar to those of powdered samples. For halloysite-(10 Å), the ethylene-glycol solvation (EG) induced a shift and a broadening of the (001) peak, from near 10 Å to 10.2–10.8 Å, whereas the diffraction band between 7.5 and 10 Å was slightly modified. In contrast, halloysite-(7.5 Å) lost its ability to regain a 10 Å-spacing. Samples 5 and 6 had an intermediate behaviour. All halloysites have shown the appearance or the strong increase of the d(002) at 3.6 Å in case of dehydration. A partially naturally dehydrated halloysite dehydrated further upon

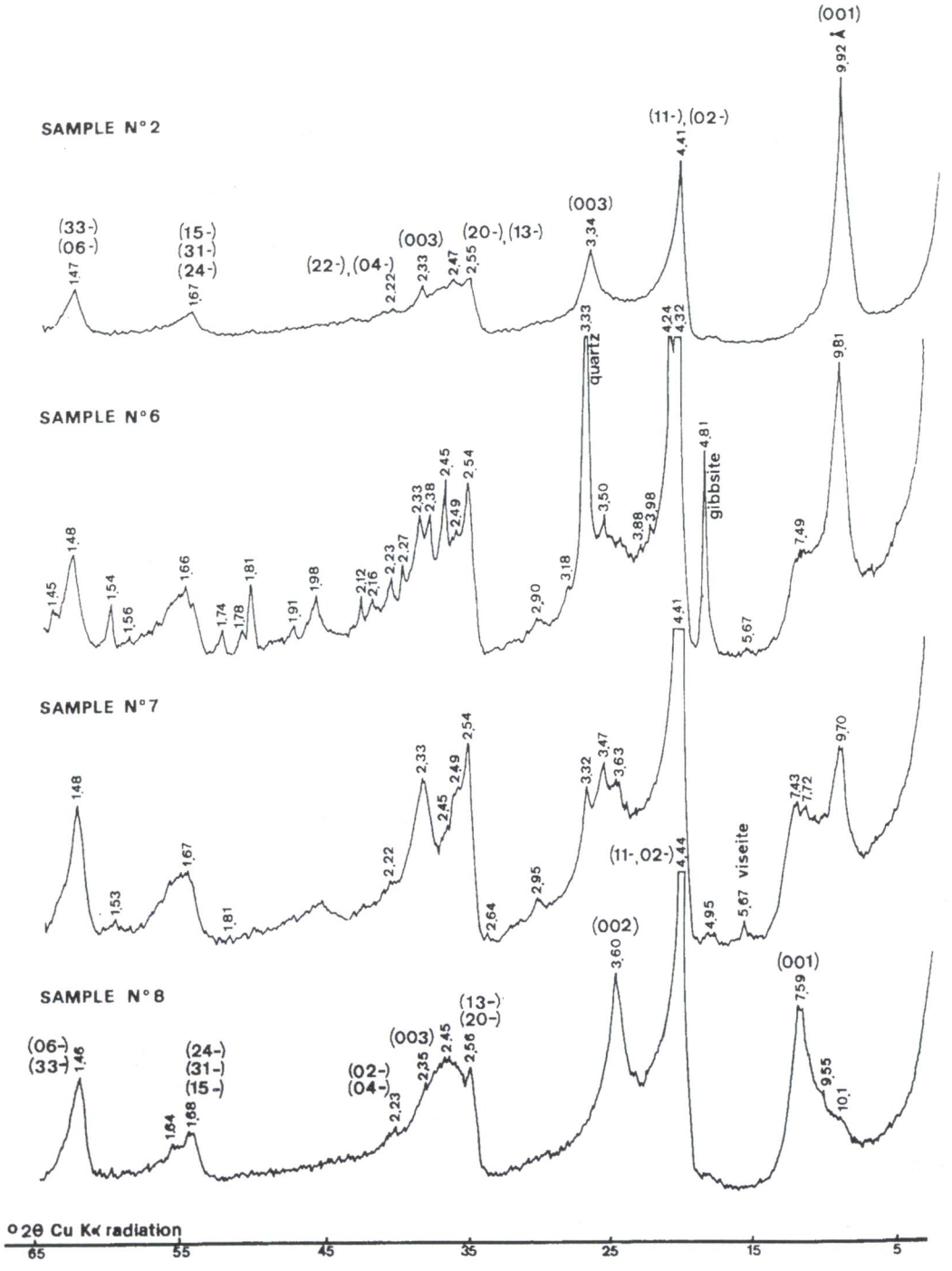

Fig. 2. X-ray powder diffraction patterns of four samples of halloysite from Angleur, covering the full range of natural hydration.

heating to 110 °C (4 hours) and exhibits a well-defined peak at about 7.4 Å. In the case of a hydrated halloysite, dehydration was not complete and led to a poorly resolved basal peak, as shown by the persistence of a hump at 10 Å (samples 2 and 5). Therefore loss of the interlayered water remained more difficult to reach for most hydrated samples. A temperature of 110 °C was not high enough to remove all the interlayered water because the latter in halloysite-(10 Å) was more strongly bounded than in partially dehydrated halloysite. Although dehydrated halloysite when heated for 1 hour to 100 °C resisted to EG treatment (Mac Ewan 1947); EG solvation, in our case, was very weak and related to an initial hydration degree, that affected both the hydrated and dehydrated layers. The retention of the interlayered water on drying varied from sample to sample. A further collapse of halloysite took place after heating to 150 °C and 300 °C;

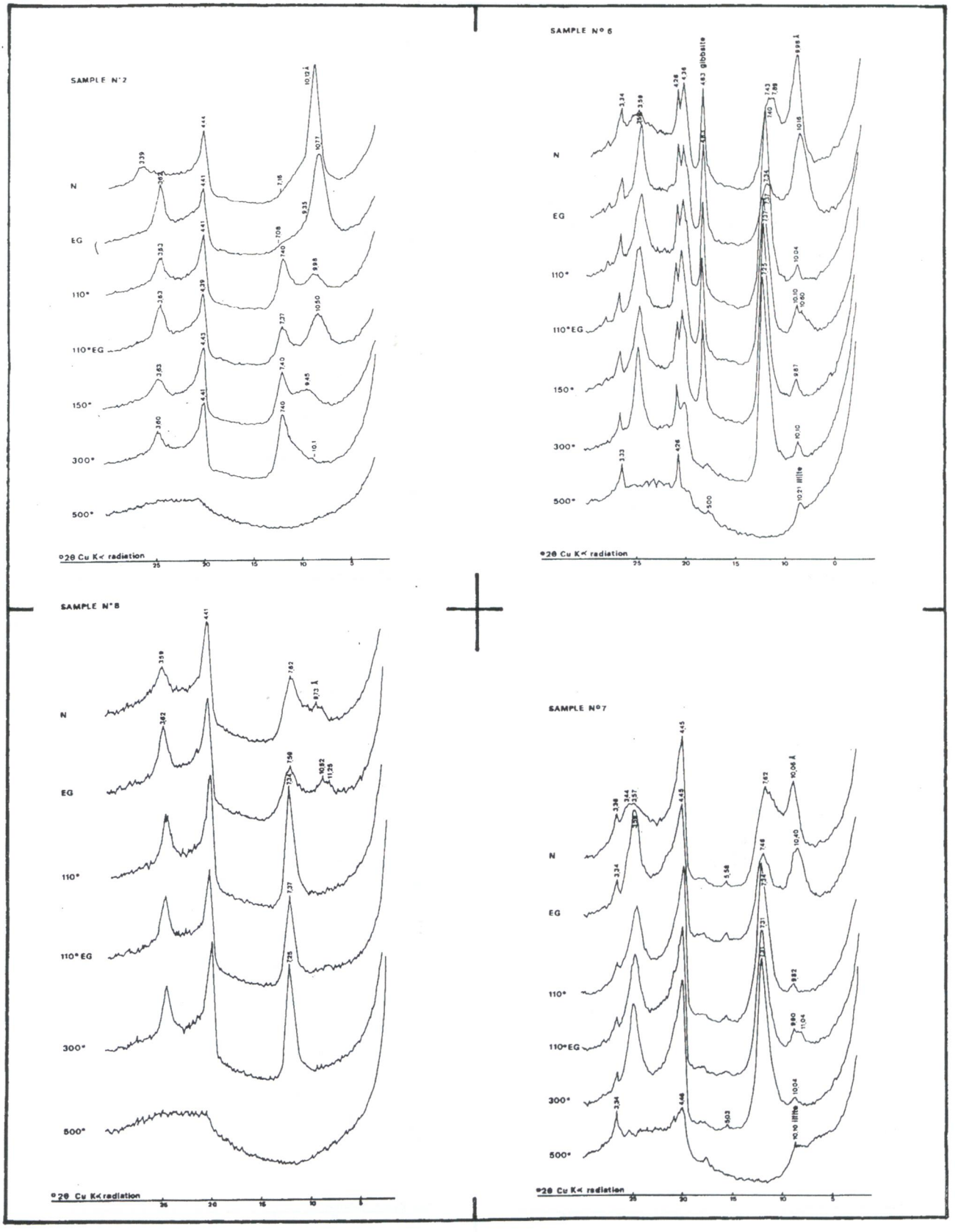

Fig. 3. XRD traces of four oriented aggregates of Angleur's halloysite, covering the range of natural hydration degree. (N): air dried at room temperature; (EG): ethylene-glycol solvated; (110˚): heated at 110 ˚C for 4 hours; (110˚EG): ethylene-glycol solvation after heating; (300˚): and (500˚): heated at 300˚C for 2 hours and at 500˚C for 4 hours, respectively.

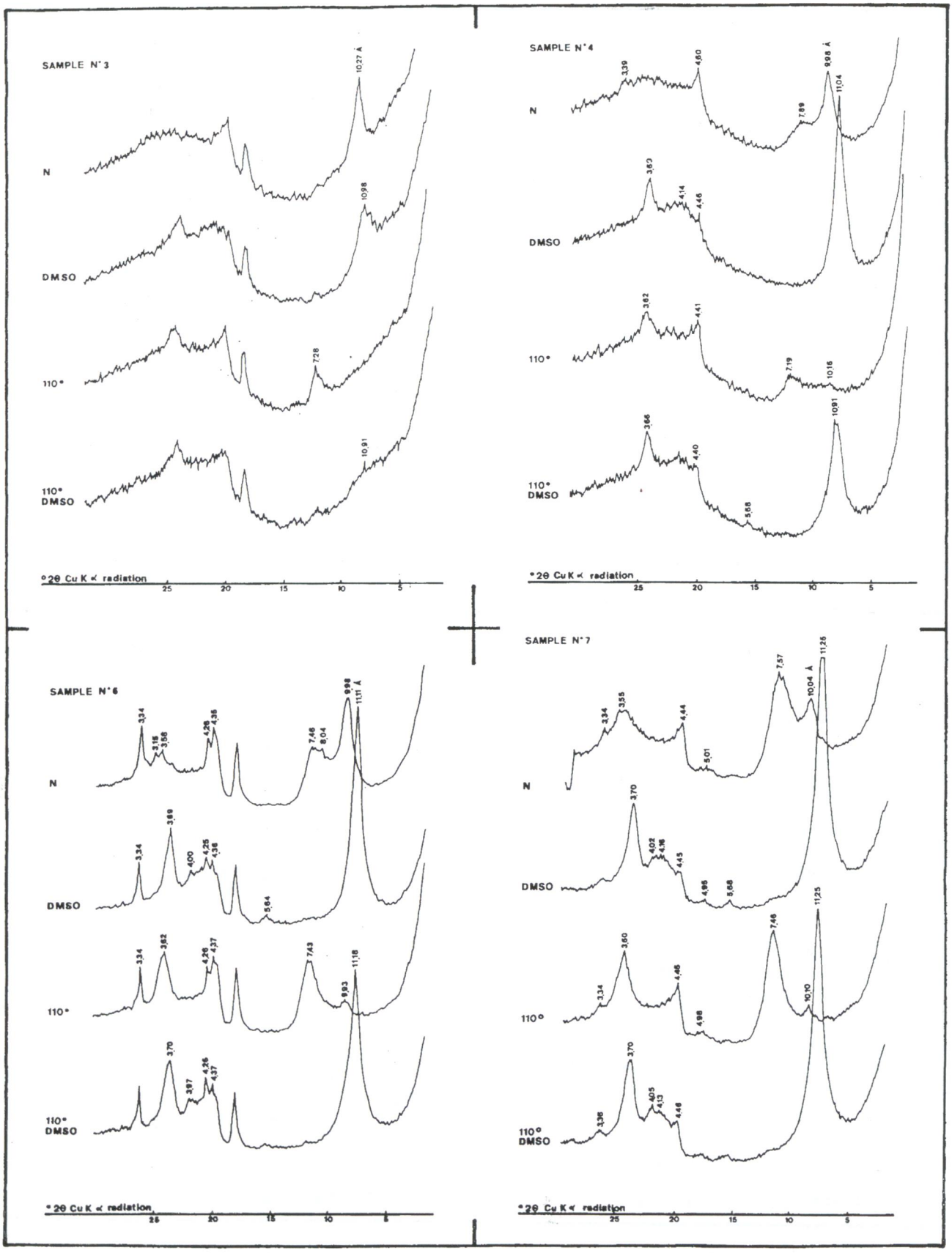

Fig. 4. X-ray diffraction patterns of basal-peak (001) of halloysite from Angleur. (N): untreated; (DMSO): treated with dimethylsulfoxide vapors; (110°): heated after DMSO solvation; (110°DMSO): DMSO reintercalated after heating.

however, dehydration of a fully hydrated halloysite (sample 2) was not complete as shown by a shoulder on the lower angle side. Brindley & Goodyear (1948) have found the necessity to heat their studied halloysites (7.5 Å) to 300 °C in order to remove completely the interlayered water. Such a removal was directly related to a) the content of water, before heating, b) the type and strength of bonding, and c) the type of dehydration. There were some differences between a dehydration state in the natural deposits, and an artificial dehydration through a radical heating obtained in the laboratory. Heating to 500 °C produced complete dehydroxylation of halloysite in all studied samples, and disappearance of the associated minerals. A 10 Å residual peak in some samples indicated occurrence of discrete illite.

Thompson & Cuff (1985) reported that a kaolinite exposed to heated DMSO vapors led to a three dimensionally ordered intercalate. Costanzo & Giese (1986) recently reported that a vapor treatment also formed an ordered intercalate with halloysite, an unexpected property because of the tubular morphology and high degree of disorder in halloysite.

Either hydrated or dehydrated halloysite easily intercalated warm DMSO (60 °C) in our case. This intercalation induced a shift of the basal reflection to 11 Å (Fig. 4); height, acuteness and shift towards the lower angle side were related to the original hydration state.

Heating to 110 °C of an ordered halloysite–DMSO–intercalate provided poorly resolved XRD patterns, especially with the most hydrated samples. When exposed to DMSO vapors, dehydrated halloysites exhibited the same XRD patterns when compared to the first saturation, but with a decreasing intensity of the 11 Å. Halloysite-(7 Å) intercalated more easily DMSO than halloysite-(10 Å), probably because of the water bonding type in the interlayered spaces that hindered good replacement of the water by organic molecules. Intercalation with DMSO of fully hydrated halloysite was accompanied by a partial structural disorganization.

The formation of a 10.8 Å-formamide intercalate has been used to differentiate kaolinite from halloysite; kaolinite intercalated formamide very slowly and only partially, while halloysite quantitatively intercalated rapidly, whatever the cristallinity, composition or shape of the particles (Churchman et al. 1984; Theng et al. 1984). Formamide treatment of halloysite (Fig. 5) induced a shift of the basal reflection to 10.8 Å, and the appearence of a third order reflection. Irrespectively of its initial hydration state, halloysite was apparently able to form complete or nearly complete interlayer complexes with formamide (Churchman et al. 1984). Formamide intercalation was not so dommageable for the structure as with DMSO; this was demonstrated by better resolved XRD patterns obtained after heating to 110 °C. Any other formamide treatment did not produce the same XR patterns, a more important part of the dehydrated particles having lost ability to intercalate formamide after the first intercalation. The reason for which each drying led to a decrease of expandibility by formamide, was not obvious; the fact that more energy was apparently required for assessing an interlayer intercalation was probably related to a structural or morphological change induced by an over-expansion.

Exposure to hydrazine vapors enabled one to produce a complete expansion of all halloysites (Fig. 6). These exhibited a very intense but narrow reflection at 10.3 Å, with an increase intensity of the (003) reflection. As already noted with DMSO intercalation, the height of the (001) reflection appeared to be proportionnal to hydration whereas dehydrazination was easier for partially dehydrated samples. Halloysite–hydrazine complexes were unstable because of the volatilization of organic liquid from the interlayered space (Theng et al. 1984). However after one night at room temperature, dehydrazination remained weak as indicated by a slight decrease of intensity of (00l) reflections and by the appearance of an asymmetry on the lower angle side.

Hydrochloric acid attack was regularly used for differentiation of kaolinites from chlorites. In XRD routine, only chlorites may be detected with some confidence (i.e. (003) at 4.7 Å in EG–XR pattern, or a clear doublet at 3.5 Å). Therefore, further tests were needed here to identify the presence of kaolinites and to estimate its relative abundance. Treatment with boiling HCl 4N during 5 minutes dissolved chlorites. Unfortunately, some Al-chlorites may offer a (variable) resistance and remain sometimes imperfectly decomposed. In practice, a differentiation between kaolinites and chlorites remains delicate. Therefore, limitations of solubility of halloysite by HCl was important. Grim (1963) mentioned that the range of solubility, for halloysite dried at a temperature of 105 to 108 °C, was 6–15% in «50%» HCl acid for 2 hours; the solubility increased with both particle size and decreasing degree of crystallinity. HCl attack was here applied to 4 samples, only the two extreme behaviours were illustrated (Fig. 7). A partial solubilization was effective by comparing the intensity of the basal reflection at 3.33 Å quartz reflection (samples 7). The most striking changes were the complete to partial dehydration (samples 7 and 2). This was illustrated for hydrated halloysite (sample 2) by an increase of the 4.44 Å reflection intensity and occurrence of a broad diffraction band between 8 and 10 Å. HCl treatment had two effects: the first corresponded to a partial solubilization (which was observed only when the clay admixture comprised HCl-resistant minerals), and the second was a dehydration.

In the present study, a complete XRD investigation has been made of the original halloysite from Angleur. Difficulties have arisen because of its heterogeneities. The structure was very labile; all the interlayers did not loose their water content at the same time as demonstrated by the gradual shift of reflections. Naturally occurring halloysites had intermediates between fully hydrated forms (10 Å) and dehydrated ones (7.5 Å). This assumption was well supported here by XRD analyses. Loss of water produced a shift of d(001) from 10 to 7.4 Å. Removal of

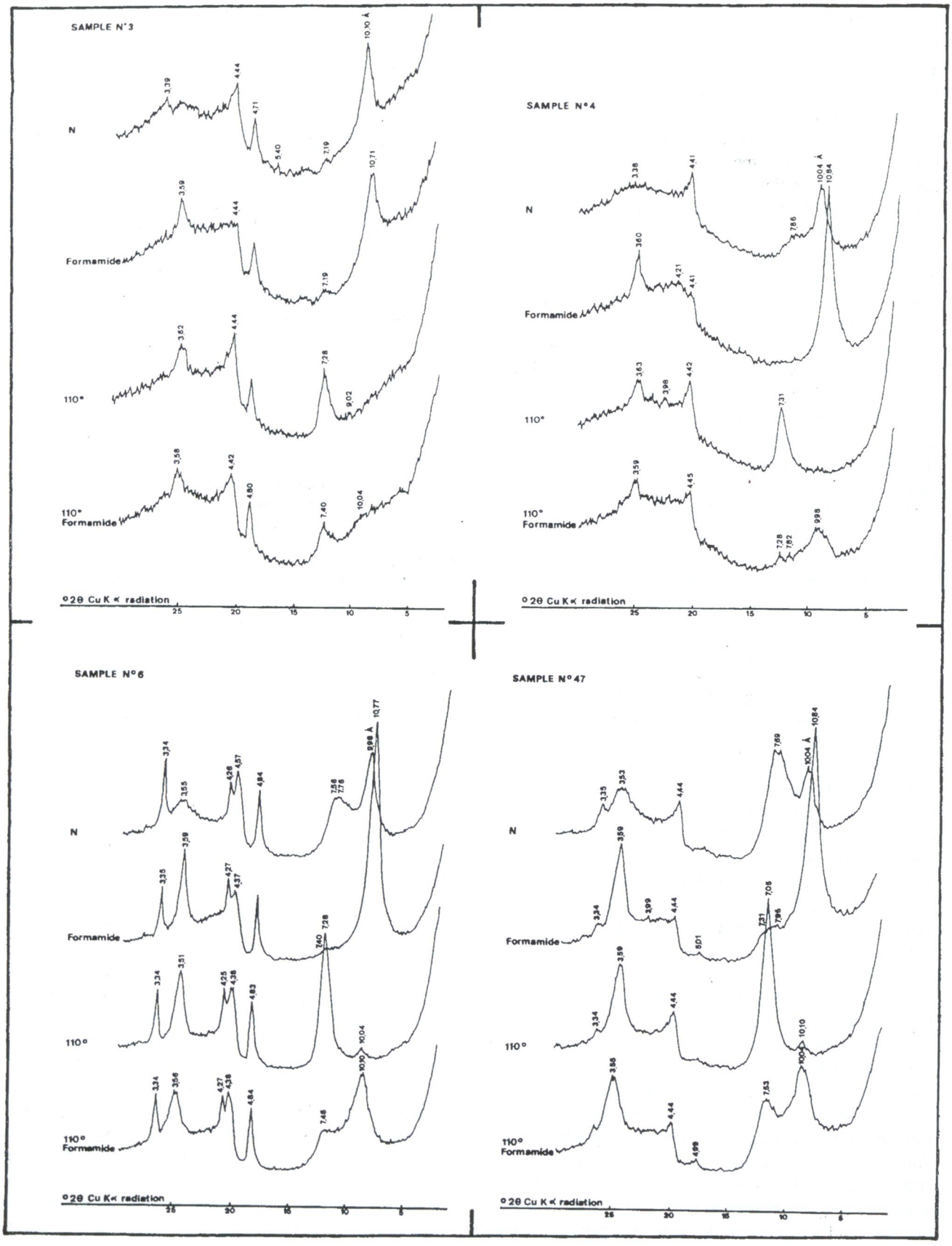

Fig. 5. X-ray diffraction patterns of basal-peak area of halloysite from Angleur. (N): untreated; (Formamide): treated with formamide vapors; (110°): heated after formamide solvation; (110°Formamide): formamide re-intercalated after heating.

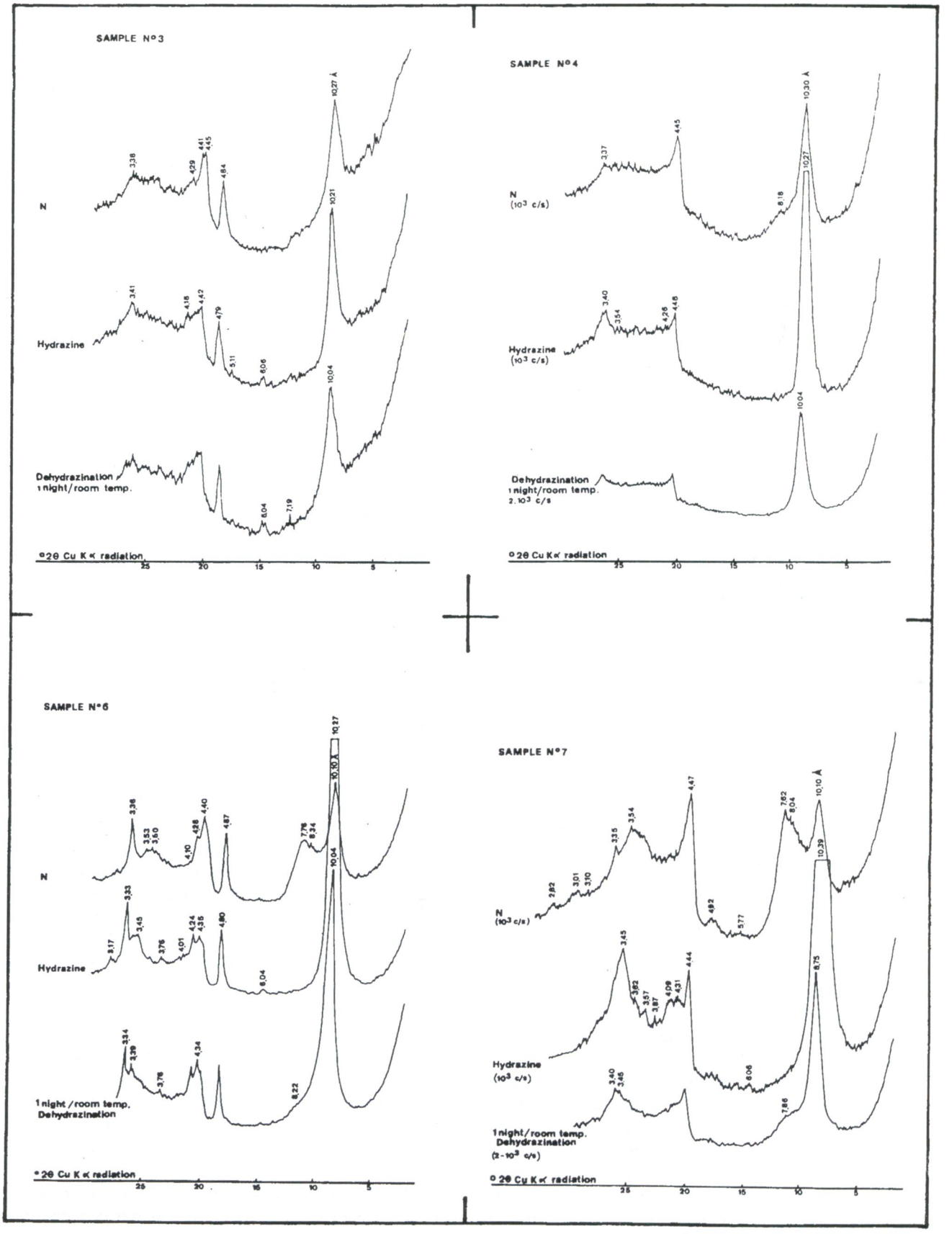

Fig. 6. XRD patterns of basal-peak area of halloysite from Angleur. (N): untreated; (Hydrazine): treated with hydrazine vapors; (Dehydrazination): naturally deintercalated, samples kept at room temperature.

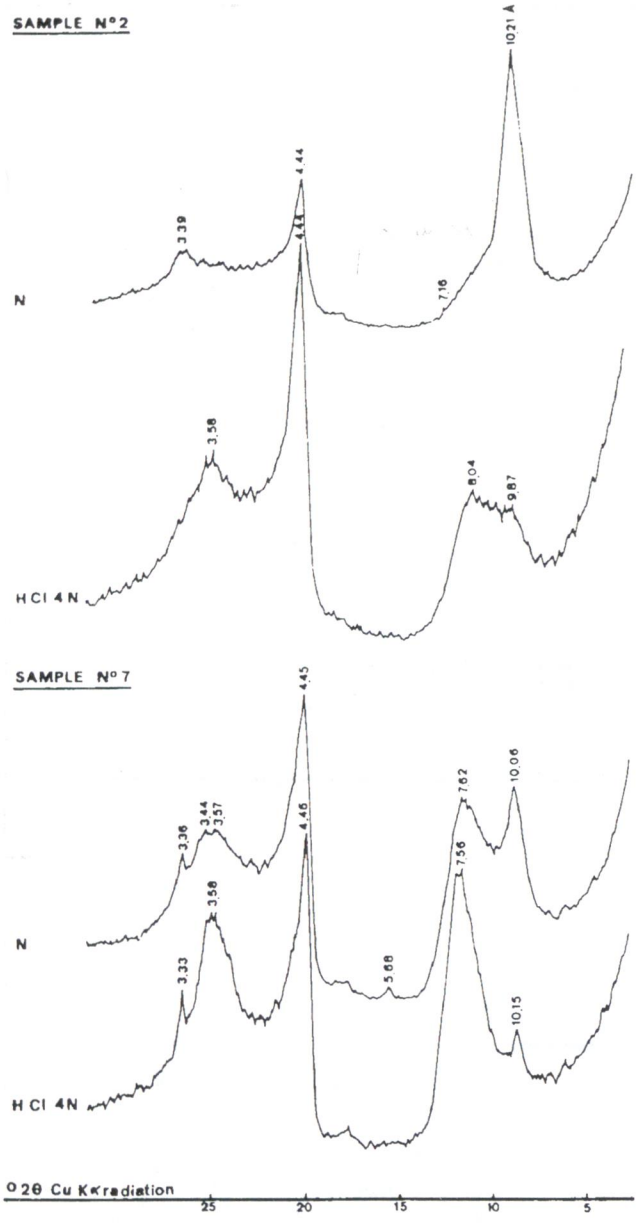

Fig. 7. X-ray diffraction patterns of two samples, before (N: untreated) and after boiling with 4N HCl for 5 minutes (HCl 4N).

water was not complete by drying in natural conditions. For fully hydrated halloysites, the process was very quick, but slower for intermediate hydration forms; the final collapse of d-spacing to 7.2 Å has required heating.

Formation of organic complexes (EG, DMSO, formamide, hydrazine) with halloysite was very easy. However EG and DMSO reacted differently depending on hydration. Formamide and hydrazine treatments were less sensitive to hydration. Subsequent deintercalation by heating and departure of organic molecules more or less strongly destabilized the structure with any further intercalation either incomplete (formamide), pratically worthless (EG) or still depending on the initial hydration (DMSO). The origin

Table 2: Variation of water content during natural dehydration in the deposit or after the laboratory storage.

SAMPLES					
1	1bis	9	10	7	8
MEGASCOPIC CHARACTERS					
porcelaneous blue color	porcelaneous blue color		grey-blue	terrous, white	porcelaneous white
STORAGE CONDITIONS					
deposit naturally hydrated	1 year room temperature laboratory storage	5 years	deposit naturally dehydrated	deposit naturally dehydrated	> 100 years room temperature laboratory
26.05% TGA	24.96% TGA	20.53% LOI	23.40% LOI 23.12% TGA	19.63% LOI 18.59% TGA 18.17% TGA	19.71% LOI 16.33% 110°C

of intercalation has puzzled some analysts. Probably, the size of the complexing agent is an important factor in determining the interlayer capacity. However, other factors are important like particle size, morphological shape, stacking disorder, proportion and nature of defects, and chemical compositions.

3. Chemical composition

Chemical analyses (Table 1) were recalculated to account for total H_2O, since published H_2O^- results were obtained by unequivalent methods. The classic differentiation between H_2O^+ et H_2O^- was worthless for a mineral loosing spontaneously its water content in a continuous way between room temperature and 150 °C.

Analyses when presented at the same level exhibited similarities between the original material studied by Berthier (1) and the most hydrated halloysite (5) recently collected in Angleur. Samples collected at Berthier's time and stored in museum, were naturally dehydrated (Giese 1988) (analyses 2 and 3). The unusually high ratio of $K_2O + Na_2O$ in analysis (3) (Richardson in Ross & Kerr 1935) was probably related to a close association with alunite. Analysis (4) (Buttgenbach 1947), was that of an impure sample shown by the anomalous content in Fe and Al. Our analysis (5) of Type–I halloysite corresponded by its morphology and chemical composition to Berthier's one. Analysis (7) of Type–II halloysite (sample 7) was in good agreement with XRD data and was characterized by a lower water content than in Type–I; analysis 6 illustrated the intermediary state.

The crystallochemical formula were calculated on the basis of 4 Si per structural unit, without taking into account Co and Zn adsorbed in the structure (Tiller & Hodgson 1962). Steinberg et. al. (1985) have found two zinciferous phases in a white halloysitic clay from Central Tunisia, with the first being a saucinite, and the second a nearly amor-

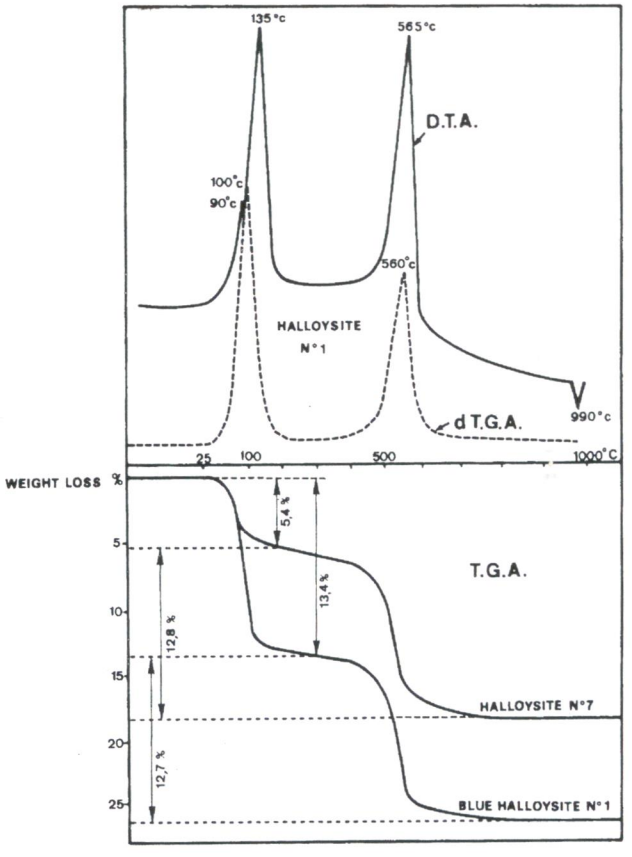

Fig. 8. DTA curve for sample 1 (fully hydrated halloysite of Type-I) and TGA curves for samples 1 and 7 (dehydrated halloysite of Type-II).

phous Zn-hydroxyde gel, halloysite; halloysite seemed totally devoid of Zn. In Angleur, traces of P and Zn have been detected by X-ray fluorescence in Type–II halloysite and allophane. P, Ti, Mn, Mg, Ca, Na and K were not considered in crystallochemical formulas, because of a content close to the detection limits, or because their role in the structure within a naturally heterogenous material was doubtful. For the same reasons, formulae are given with two decimals. The crystallochemical formulas are:

$Al_{4,03}\ Si_{4,00}\ O_{10}\ (OH)_8$. 4,78 H_2O (analysis 5);
$Al_{3,92}\ Si_{4,00}\ O_{10}\ (OH)_8$. 3,49 H_2O (analysis 6);
$Al_{3,74}\ Si_{4,00}\ O_{10}\ (OH)_8$. 1,91 H_2O (analysis 7).

If we accept Si for Al substitution, on the basis of 8 (Al + Si) (analysis 5), the formula was $Al_{4,01}\ Si_{3,99}\ O_{10}\ (OH)_8$. 4,75 H_2O. Even then analysis (5) has an excess of water, which was probably due to trapped water in the porcelaneous masses, a fact in good agreement with Chukhrov & Zvyagin (1966). Analyses 6 and 7, on the basis of 4 Si, gave an unexpected deficit in Al. This could be contradictory with the observations of Ross & Kerr (1935), but one cannot exclude the presence of amorphous silica-rich compounds. The discrepancy in the H_2O ratio between Type–I and Type–II halloysites was accompanied by a variation in the same trend for Al in minerals with higher Al/Si ratios.

X-ray spectrography indicated only traces of Pb and As. Mössbauer spectroscopy determined the oxydation state of iron: Fe^{3+} was the major valence state with Fe^{3+}/Fe^{2+} ratio being greater than 0.80. The origin of the blue color of Type-I halloysite has been investigated. Trace elements detected in the halloysite like Cr^{3+}, Ni^{2+} (Vernet 1962) and Co^{2+} may induce a blue color. If Ni was an unfrequent contributor in minerals, it was usually present as Ni^{2+} in octahedrals and induced a green color (Rossman 1988). Our study did not reveal the cause, because the lack of knowledge about the exact status of these cations either inside or outside the halloysite structure, although the Al^{3+} by Cr^{3+} substitution has been illustrated by Maksimovic & White (1972), in the case of a blueish halloysite.

4. Thermal Analysis

DTA (differential thermal analysis), TGA (thermogravimetric analysis) and dTGA (derived TGA) curves are illustrated in figure 8 and in Table 2. No other phases than halloysite were detected by DTA. The DTA curve of halloysite usually has two main V-shaped endothermic peaks at 135 and 565°C, and an exothermic peak at 990 °C. The loss of water at 135 °C, associated with the collapse of the halloysite lattice was clearly observed by DTA. The size of the 135 °C peak was directly related to the degree of hydration. The structure of halloysite-(10 Å) (Giese 1988) agreed for an interlayered water divided into equal populations. Distinction between the two types of interlayer water (hole water and associated water) was found in their different positions and interlayer bonds; the hole water was more stable than the associated water. Ordered halloysites exhibited a more rapid loss of associated water than the hole water, whereas for more disordered samples, there is less distinction between the two types of water, because of the lost of interlayered water in an apparently continuous manner (Giese 1988). This was in agreement with a discreet endothermic peak at 90°C only for Type–I halloysite. In all the cases the dTGA curve related to the speed of weight loss, has shown a major peak at 100°C. A further collapse of the halloysite c-parameter to about 7.40 Å took place when the material was heated to 300°C for 2 hours at least. This loss of water was evident on the TGA curves by a slope between the two more important removal processes of water, and on XRD patterns by the persistence of an asymmetry on the lower angle side of the 7.40 Å reflection. The endothermic peak at 565°C was due to dehydroxylation. In agreement with Kirkman (1980), the high temperature at which our halloysite-(10 Å) dehydroxylation took place, indicated a well ordered mineral. The high temperature exothermic reaction (990°C) reported by Minato (1965) corresponded to the formation of gamma–alumina.

Weight losses were measured quantitatively, and TGA curves were obtained for halloysite-(10 Å) and halloysite-

Table 3: Cation exchange capacity for halloysites in decreasing order of hydration degree.

Type-I blue halloysite	45.6
Type-II white halloysite (sample 7)	22.7
Dehydrated halloysite (sample 8, museum storage)	18.9
110 °C heated halloysite	10.4
CEC in milliequivalents by 100 g.	

(7.5 Å) (Fig. 8). The loss of weight due to the removal of interlayered water was directly related to the hydration degree. Halloysite-(7.5 Å) still contained 5.37% of water, which agreed with X-ray and chemical data. The loss of weight by dehydroxylation was about 12.8% for the two investigated halloysites.

5. Cation Exchange Capacity

Table 3 listed CEC for four samples. Type–I halloysite and the heated halloysite have values matching fully hydrated and dehydrated halloysites respectively (Grim 1963). Halloysites 7 and 8 had closer CEC values, which were intermediate between the two extreme states of dehydration, a property supported by XRD, chemical and thermal analyses.

6. Infrared Spectroscopy

Due to the complex composition, assessment and explanation of all absorption bands were not completed. Sharp bands indicated a low degree of disorder in the lattice, in agreement with the low substitution rates in the halloysite from Angleur, therefore, the spectrum was believed to be quite representative of an ideal halloysite.

Stubican & Roy (1961), Maksimovic & White (1966), and Elsass & Oliver (1978) assigned the 790 cm^{-1} band to a Si–O vibration, and the 750 to 535 cm^{-1} bands to Al–O–Si vibrations. The lower Al content in halloysite Type–II was illustrated by the decreasing intensity of the 750 cm^{-1} band and a light shift of 5 cm^{-1} for the Si–O–Al bands towards a higher frequency.

In the region between 1200 and 800 cm^{-1}, halloysite showed bands at 1080, 1038 and 910 cm^{-1}. The two first have been assigned to an antisymmetric streching mode of Si–O–Si bands, and the last to an Al–OH bending mode. The lack of shift of the major Si–O band (1038 cm^{-1}) towards low wave numbers, between Type–I and Type–II halloysites, were consistent with the lack of replacement in both tetrahedral and octahedral sheets (Maksimovic & White 1966; Wada et al. 1988).

In the region corresponding to the stretching modes of water, halloysite-(10 Å) showed only distinct absorption bands at 3695 and 3621 cm^{-1} (Van der Marel & Krohmer 1969); the spectrum undoubtedly showed the presence of water molecules and hydroxyl groups even after drying 4 hrs at 110 °C. In good agreement with the X-ray diffraction observations, halloysite could not be entirely dehydrated at this temperature. The dehydration of Type–I halloysite was illustrated by a weakening of 3550, 3475 and 3420 cm^{-1} bands which collapsed into a single but broad band around 3490 cm^{-1}, and by the decreasing intensity ratio of 3695 cm^{-1}/3621 cm^{-1}. The most natural dehydrated material (sample 7 (c)) exhibited the same spectrum as for the artificially dehydrated halloysite (b).

7. Optical properties

The optical properties of halloysite-(10Å) (Type–I) are: Ng = 1.530(2), Nm = 1.528(2), Np = 1.523(2), with a negative optic sign, tubes had a positive elongation and a medium 2V angle of 64° (calc.). After one minute of immersion in index liquids, especially if the sample had been kept in the air, one observed a quick «invasion» of the grains by the immersion liquids, this phenomenon was clearly illustrated by a gradual shift of color and change of refractive indices. The influence of immersion media on optical properties depended on the nature of the organic molecules and on the hydration rate of halloysite. The refractive indices of halloysite increased with time, after absorption of organic molecules and loss of water. This confirmed Grim's assumptions (1963) that organic compounds were most likely to significant cause of variations in the optical characteristics of halloysite containing more than $2H_2O$. Van Baren (1936) investigated the influence of various organic liquids and had found no changes in the indices of kaolinite and «halloysite $2H_2O$». This was not unexpected, because the generally absorption of organic molecules correlated with the hydration rate. The interference figure is rather unexpected also because of the usually low degree of crystallinity and extremely small sizes of halloysite. However, in this study, Type–I halloysite exhibited in plain light a fibrous texture composed by bundles of fibers with simultaneous extinctions under crossed nicols. Preferential orientations of compact pseudohexagonal rod aggregates were consistent with slickensides and SEM observations. Halloysite tubes, 1 to 3 microns in length, underlined scarce shallow cavities with a diameter of 15–25 µm which were distributed in the halloysite mass. We have compared such tubes with those observed by TEM by Degueldre & Dekeyser (1954) of a partially dehydrated halloysite from Angleur, with XRD characteristies similar to that of sample 6.

Because most of the halloysite-(7.5 Å) (sample 8) appeared isotropic with a mean index in the range of 1.546–1.550, only the mean indices of refraction have been measured. However, more organized islands with a weak birefringence persisted. This confirmed that sample 8 derived from a blue halloysite-(10 Å) after room dehydration. The range of indices, was in good agreement with the value of 1.552 measured by Ross & Kerr (1935) in a dehydrated specimen (cf. analysis (3), Table 2) and showed that samples

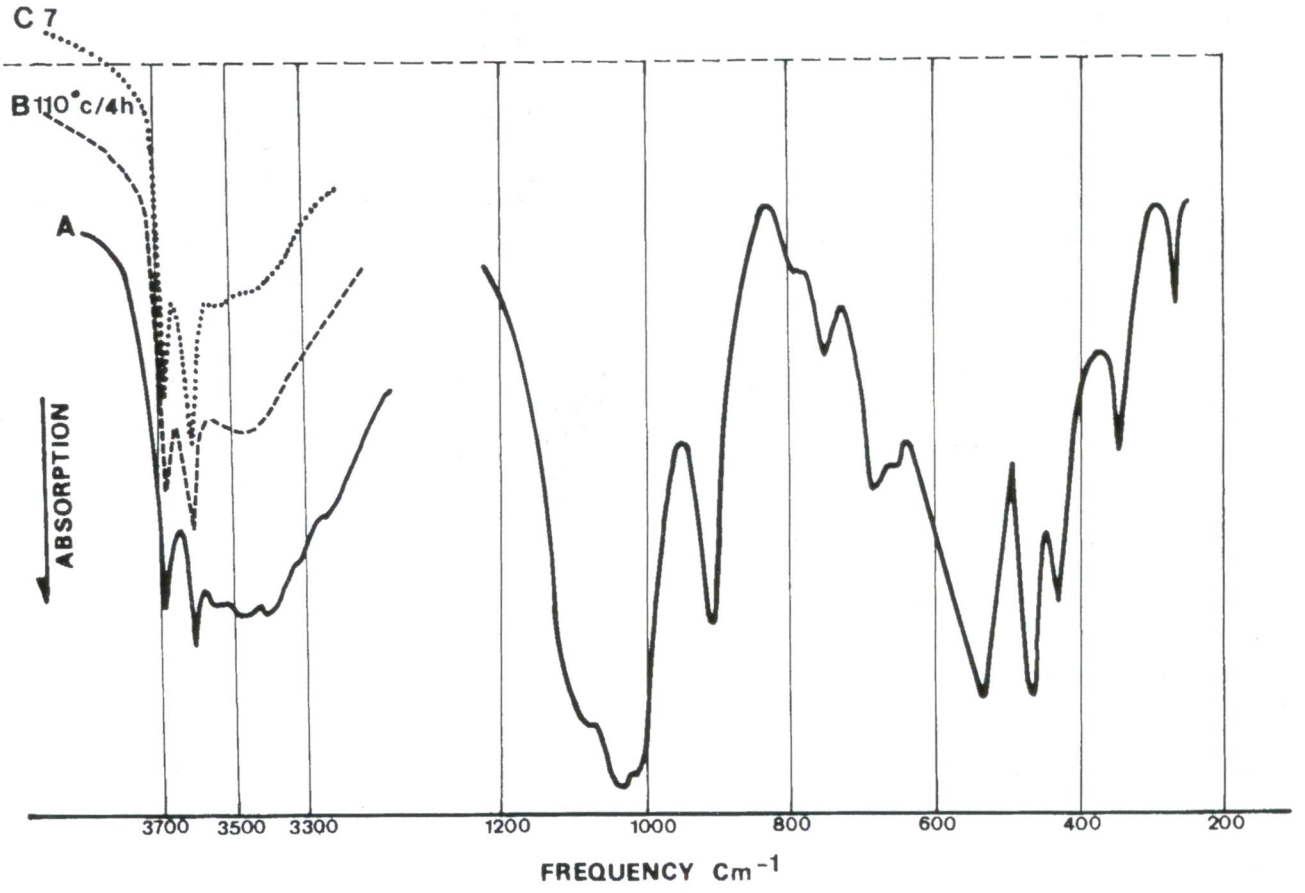

Fig. 9. IR absorption spectra. (A) porcelaneous blue halloysite, Type-I; (B) blue halloysite heated at 110 °C for 4 hours; (C) dehydrated halloysite, sample 7, Type-II. IR absorption spectra B and C are quite similar to A and are not represented in the frequency between 1200 and 200 cm^{-1}.

collected at Berthier's time and preserved in collections have reached the same state of dehydration. In agreement with Grim (1963) and Bonatti & Gallitelli (1950), transition from a hydrated to a dehydrated form was accompanied by an increase of the mean refractive index.

SEM observations of sample **7** revealed a loose aggregate of granules, 3 to 10 μm in diameter, composed of interlacing spatula-like tubes. This morphology induced the high porosity of the chalky halloysite-(7.4 Å). Naturally but partially dehydrated halloysite was characterized by dominant short rods with a length from 0.2 to 0.5 μm.

Genetic aspects

The precise process description of the halloysite genesis is limited by current observation conditions. Ross & Kerr (1935) wrote: «all the deposits are exhausted and it is impossible to obtain material from the old mine openings». The mining site is closed since more of a century and geological detail contacts non longer are visible. Alone the global geological context and the comparison with equivalent geological contexts is allowed. Ross & Kerr (*op. cit.*) were first and alone to have tried to tackle the genetic aspects: «the halloysite from Liège, Belgium, is known to come from a region of old zinc mines, and its association with alunite makes it seems probable that sulfuric acid solutions have played a part in producing the halloysite of that region». More recently, geological conditions similar to those of Angleur were discribed in the literature: in karstic system developed within a limestone host-rock (Gulinck & Dekeyser 1957; Martin Vivaldi & Girela Vilchez 1958; Keller et al. 1966; Ertus et al. 1989); in limestone in contact with black shales or other organic-rich sediments (Steinberg et al. 1985); with occurrence of disseminated sulfides or orebodies (Steinberg et al. 1985). Some among these authors have suggested that halloysite has been formed in an acid environment through oxydation of sulfides; halloysite has resulted from supergene processes due to acid-bearing solutions reacting with parent illitic minerals. In the Belgium Ardennes (Entre–Sambre–et–Meuse), halloysitic masses were found in karstic cavities crosscuting Paleozoic limestones. These caves have been filled with Oligocene sands and Miocene lignitic sediments. The detailed study of one of these settings (Weillen's sink) allowed to explain the genesis of halloysitic claystones by oxidation of pyrite, through percolation of sulfuric waters, clay hydrolysis

Table 4: Association scheme for clay samples from Angleur.

	Source rock – Halloysite – Increased weathering
ILLITE	———– – – – .....
HALLOYSITE-(10Å)	———– .....
HALLOYSITE-(7Å)	———– .....
ALUNITE	.....
ALLOPHANE	..... ———–
VISEITE	———–
ALUMOHYDROCALCITE	———–
GIBBSITE	..... ———– .....
QUARTZ	———– ..... ———– .....

___: present to abundant; – – – –: occasional; .....: rare or absent

and alumina leaching led to forming halloysite within a bedrock composed of silicified limestone. The genesis resulted from a combination of the leached alumina and the silica produced by limestone dissolution (Ertus et al. 1989).

In the case of Angleur, sulfides fault have been certainly the main source for acidity (sulfuric acid solutions have played a role in the mineral genesis and karstification); however we may not completely totally exclude the contribution of pyrite-bearing Namurian black shales. The source-rock for Al and Si was mainly a residual material, presumably derived from the leaching of 'illite' and kaolinite from Namurian black shales, with the possible contribution of dissolved limestone material or of overburden trapped in karst cavities. 'Illites' of Namurian shales are a mixture of non-expandable illite and a random illite-smectite mixed-layer (with less than 15% smectitic layers). Traces of illite, identified by XRD after heating the sample at 500°C, might point to a relic of this parent material. Occurrence of halloysite with different hydration states, was consistent with the metastable nature of the mineral (Giese 1988; Huang 1974). The «in situ» dehydration depended on the water table level and was accompanied by morphological and chemical changes, as indicated by the appearance of allophane, viseite, alumohydrocalcite and gibbsite (Table 4). Very similar mineral associations have been described in the Visé area (20 km, east of Angleur) where karstic phenomena have affected Visean limestones (Melon et al. 1976); viseite was in close association with amorphous P-bearing compounds (allophane, evansite, delvauxite). It seems probable that, in Angleur area, P needed by viseite originated from allophane. Calcium in viseite and alumohydrocalcite and carbonate in alumohydrocalcite derived from the limestone environment. The end-products of halloysite weathering were in close association with such compounds and with gibbsite and quartz.

Conclusions

The studied material, with a similar origin, chemical composition and morphology to the original halloysite found by Berthier (1826), may be considered equivalent to the type material. Therefore, the re-examination of halloysite from Angleur enabled us to present new data for the type-locality. The need for a complete investigation also came from the natural unstability of the mineral, which resulted in the transformation of Berthier's type material, and from the disparity of the scarce results so far published. X-ray, chemical, optical, and thermal analyses of halloysite show a strict dependence of results accordingly to the hydration degree and the continuous transition of halloysite-(10 Å) to halloysite-(7 Å).

Acknowledgements: The authors would like to thank Prof. Dr Jacques Thorez, for his critical comments and reviews on the manuscript, the editor and the referees for their comments, suggestions and for reviewing the English phraseology. Thanks are due to the staff of the General Geology Siliciclastic Sedimentology and Clay Crystallogenesis Laboratory of Liège University.

References

Berthier P., 1826: Analyse de l'halloysite. *Ann. chim. et phys.*, 32, 332–335.

Bonatti S. & Gallitelli P., 1950: Metahalloysite nelle farine fossile di Bagnoregio (Viterbo). *Atti della Societa Toscana di Scienze Naturali residente in Pisa. Memorie*, 57 – série A, 3–10.

Brindley G.W. & Goodyear J., 1948: X–ray studies of halloysite and metahalloysite. *Min. Mag.*, 28, 407–422.

Buttgenbach H., 1947: Les minéraux de Belgique et du Congo belge. *Ed. Vaillant–Carmanne, Liège–Dunod, Paris*, 1–573.

Calembert L., Pel J., Monjoie A., Burton E. & Lambrecht L., 1974: Les guides scientifiques du Sart Tilman. *Conseil scientifique des sites du Sart Tilman, Liège, n°1, Géologie*, 1–107.

Chukhrov F.V. & Zvyagin B.B., 1966: Halloysite, a crystallochemically and mineralogical distinct species. *Proceed. Intern. Clay Conf., Jerusalem, Israël*, 11–25.

Churchman G.J., Whitton J.S. & Claridge G.G.C., 1984: Intercalation method using formamide for differentiating halloysite from kaolinite. *Clays Clay Min.*, 32, 241–248.

Constanzo P.M. & Giese R.F., 1986: Ordered halloysite–dimethylsulfoxide intercalate. *Clays Clay Min.*, 34, 105–107.

Davreux C., 1833: Essai sur la constitution géognostique de la province de Liège. *Mém. Acad. Roy. Belg., Mém. cour. in* 4°, 9.

Dekeyser W.L. & Degueldre L., 1954: Note sur les rapports entre la morphologie et la structure des kaolins et des halloysites. *Bull. Soc. belg. Géol.*, 63, 100–110.

Elsass F. & Oliver D., 1978: Infra red and electron spin resonance studies of clays representative of the sedimentary evolution of the Basin of Autun. *Clay Min.*, 13, 299–308.

Ertus R., Dupuis C. & Trauth N., 1989: Un nouveau type d'accumulation minérale de surface par épigénie d'altération météorique: halloysitisation sous couverture dans un karst sur calcaire silicifié (Belgique). *C. R. Acad. Sci., Paris*, 309, série II, 595–601.

Giese R.F., 1988: Kaolin minerals: structure and stabilities. Hydrous Phyllosilicates. *Min. Soc. Amer., Reviews in Mineralogy*, 19, 29–66.

Grim R.E., 1953: Clay mineralogy. *Mc Graw–Hill (Ed.) New York*, 384 p.

Gulinck M. & Dekeyser W., 1957: Le gisement d'halloysite de Blaton. *Bull. Soc. belg. Géol.*, 66, 381–389.

Kirkman J.H., 1980: Mineralogy of the Kauroa ash formation of south–west Waikito, North Island, New Zealand. *N. Z. Journal Geol. Geophy.*, 23, 1, 113–120.

Huang W.H., 1974: Stabilities of kaolinite and halloysite in relation to weathering of feldspars and nepheline in aqueous solution. *Amer. Min.*, 59, 365–371.

Keller W.D., Preston Mc Grain, Reesman A.L. & Saum N.M., 1966: Obsevations on the origin of endellite in Kentucky, and their extension to «indianaite». *Proceed. 13th Nat. Conf. Clays Clay Min.*, 107–120.

Lambrecht L. & Swinnen J., 1958: Compte rendu de l'excursion du 28 juin 1958 dans la région d'Angleur. *Ann. Soc. Géol. Belg.*, 81, B521–528.

Lambrecht L., 1958: Notes sur la constitution du massif namurien d'Angleur (Province de Liège). *Ann. Soc. Géol. Belg.*, 81, B223–238.

Lechatellier H., 1887: De l'action de la chaleur sur les argiles. *Bull. Soc. Fr. Min.*, 10, 204–204.

Mac Ewan D.M.C., 1947: The nomenclature of the halloysite minerals. *Min. Mag.*, 28, 36–44.

Maksimovic Z. & White J.L., 1972: Infrared study of chromium–bearing halloysites. *Proceed. Intern. Clay Conf., Madrid*, 61–73.

Martin Vivaldi J.L. & Girela Vilchez F., 1958: A study of the halloysite from Maazza (North Morocco). *Journées Internationales d'Etude des Argiles. Silicates Industriels. Association belge pour favoriser l'étude des verres et des composés siliceux*, 1–7.

Melon J., Bourguignon P. & Fransolet A.–M., 1976: Les minéraux de Belgique. *G. Lelotte (Ed.), Dison, Belgique*, 280 p.

Minato H., 1965: Dehydration curves of kaolin minerals, especially in hydrated halloysite. *1st Intern. Thermal Analysis Conference*, 199–199.

Ross C.S. & Kerr P.F., 1935: Halloysite and allophane. *U.S. Geol. Surv., Prof. Paper*, p. 185–G–185.

Rossman G.R., 1988: Optical spectroscopy in spectroscopic methods in mineralogy and geology. *Reviews in Mineralogy*, 18, Hawthone F.C. (Ed.), 207–254.

Steinberg M., Rautureau M. & Riviere M., 1985: Analysis of zinciferous clays from Central Tunisia using a scanning transmission electron microscope (STEM). *Chem. Geol.*, 48, 157–164.

Stubican V. & Roy R. (1961): Isomorphous substitution and infrared spectra of the layer lattice silicates. *Amer. Min.*, 46, 32–51.

Splichal J., 1919: Contribution to the knowledge of colloidal clays. *Zemědělský Archiv., Prague*, 10, 413, *in* Min. Abstr., 1, 288–288.

Swinnen J., 1958: Observations sur la tectonique des massifs de Streupas et de Kinkempois. *Ann. Soc. Géol. Belg.*, 81, B209–221.

Theng B.K.G., Churchman G.J., Whitton J.S. & Claridge G.G.C., 1984: Comparison of intercalation methods for differentiating halloysite from kaolinite. *Clays Clay Min.*, 32, 249–258.

Thomson J.G. & Cuff C., 1985: Crystal structure of kaolinite: dimethylsulfoxyde intercalate. *Clays Clay Min.*, 33, (6), 490–500.

Tiller K.G. & Hodgson J.F., 1962: The specific sorption of cobalt and zinc by layer silicates. *9th National Conference on Clays Clay Min.*, 9, 393–403.

Van Baren F.A., 1936: Veber den Einfluss verschiedener flüssigkeiten auf den brechungsindex von tonmineralien. *Z. Krist.*, 95, 464–499.

Van der Marel H.W. & Krohmer P., 1969: O–H stretching vibrations in kaolinite, and related minerals. *Contrib. Min. and Petrol.*, 22, 73–82.

Vernet J.P., 1962: L'halloysite bleue du Mont Vuache (Savoie). *C.R. Acad. Sc., Paris*, 254, 2377–2379.

Wada K., 1967: A study of hydroxyl groups in kaolin minerals utilizing selective deuteration and infrared spectroscopy. *Clay Min. Bull.*, 7, 51–61.